Measurement of the Surface Strain Induced by Reconstructed Surfaces of GaAs (001) Using Photoreflectance and Reflectance-Difference Spectroscopies

L. F. Lastras-Martínez,[1,*] J. M. Flores-Camacho,[1] A. Lastras-Martínez,[1] R. E. Balderas-Navarro,[1,2] and M. Cardona[3]

[1]*Instituto de Investigación en Comunicación Optica, Universidad Autonóma de San Luis Potosí, Alvaro Obregón 64, San Luis Potosí, México*

[2]*Facultad de Ciencias, Universidad Autonóma de San Luis Potosí, Alvaro Obregón 64, San Luis Potosí, México*

[3]*Max-Planck-Institut für Festkörperforschung, Heisenbergstrasse 1, 70569 Stuttgart, Germany*

(Received 7 June 2005; published 2 February 2006)

We report photoreflectance-difference and reflectance-difference measurements on reconstructed GaAs (001) surfaces. From these data the linear and quadratic electro-optic coefficient spectra are determined in the important 2.8–3.4 eV spectral region. The surface strain and fields induced by the surface reconstruction are also determined. We show experimentally that between $c(4 \times 4)$ and (2×4) surfaces, there is an inversion of the surface electric field which we attribute to a direct piezo-electric effect related to the surface strain induced by reconstruction.

DOI: 10.1103/PhysRevLett.96.047402 PACS numbers: 78.66.Fd, 78.20.−e, 78.90.+t

GaAs (001) surfaces are very important templates for the growth of nanostructured devices. Nondestructive probes, such as optical ones, are therefore of prime importance to study the complex phenomena associated with such surfaces. Reflectance-difference spectroscopy (RDS) and photoreflectance difference (PR-D) spectroscopy are two complementary techniques that have been used for the characterization of GaAs (001) surfaces [1–7].

For normal incidence on the (001) surface [in what follows, we will limit our discussion to light incident on a (001) crystal surface] RDS measures the difference in reflectivity between [110] and $[1\bar{1}0]$ light polarizations [8]. RD spectra exhibit important contributions associated with mechanical strains and surface reconstructions [4–7].

PR-D spectroscopy measures the difference between the sample photoreflectance (PR) spectrum for light polarized along (110) and the corresponding spectrum for unpolarized light [1]. PR-D is a very sensitive tool for the characterization of the surface electric field associated to band bending (for values down to 10^3 V/cm) [2] and for the study of the piezo-optical properties of semiconductors [3]. For crystals of zincblende symmetry (T_d) PR-D spectra involve only a linear electro-optic (LEO) component as, for this symmetry, the quadratic electro-optic (QEO) PR component is isotropic [1].

The physical origin of the PR LEO spectrum has been related to a piezo-optic effect induced by the electric field associated to surface band bending [1]. This electric field leads to an anisotropic strain that changes crystal symmetry from cubic to orthorhombic. When crystal symmetry is reduced, as in the case of an external stress applied along [110], the PR QEO component becomes anisotropic as well [9].

In this work we report on both PR-D and RD measurements on reconstructed GaAs (001) surfaces. By combining both techniques, it is shown that surface reconstruction leads to a surface piezo-electric field that changes sign upon conversion from $c(4 \times 4)$ to (2×4) reconstruction. Such piezo-electric field adds to the space-charge field associated with impurity ionization.

The samples used were grown by molecular-beam epitaxy on n-doped (10^{18} cm^{-3}) GaAs (001) substrates. They consist of a homoepitaxial undoped GaAs buffer layer (0.3 μm) capped with an As_2 protective layer (70 nm) deposited from an As decomposition source. After growth, the samples were transferred in air to the ultra-high-vacuum chamber equipped with PR-D and RD spectrometers and a rotating analyzer-based ellipsometer [10]. The optical measurements can be performed in the 150–800 K temperature range.

The $c(4 \times 4)$ and (2×4) reconstructed surfaces were obtained by annealing the samples at 370 and 490 °C, respectively, in order to desorb the As cap layer [11]. The As desorption process was monitored *in situ* by ellipsometry at ~2.8 eV to obtain the $c(4 \times 4)$ surface. In order to monitor changes in reconstruction from $c(4 \times 4)$ to (2×4), RDS was recorded at ~2.8 eV since at this energy RDS for both reconstructions has opposite signs [5]. For RDS the symmetries of both reconstructions were checked by reflection high-energy electron diffraction technique. After performing these measurements, the crystal directions were determined *ex situ* by chemical etching with KOH. In the present experiments the PR-D measurements were carried out with light polarized along the larger direction of the oval pits, i.e., parallel to [110] crystallographic axis [12].

Figure 1 shows PR spectra in the energy range from 2.85 to 3.25 eV for (a) $c(4 \times 4)$ and (b) (2×4) surface reconstructions of GaAs (001). This energy range corresponds to the E_1 and $E_1 + \Delta_1$ transitions. The dashed lines represent spectra taken with linearly polarized light along [110], whereas the solid line represents spectra taken with unpolarized light. The experimental results are summarized as follows: (1) The strength of the transitions is reversed upon

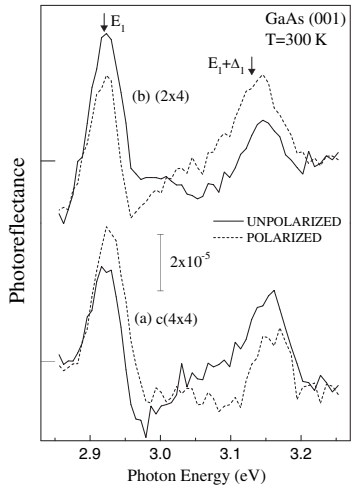

FIG. 1. PR spectra for (a) $c(4 \times 4)$ and (b) (2×4) of GaAs (001). The spectra represented by dashed and solid lines were taken with polarized light along [110] and with unpolarized light, respectively. For $c(4 \times 4)$ [(2×4)], As dimers are parallel (perpendicular) to the probe light polarization.

reconstruction; i.e., the E_1 peak in Fig. 1(a) has a smaller amplitude for the unpolarized spectrum than for the polarized one, whereas the opposite is observed for the (2×4) reconstruction as seen in Fig. 1(b). A similar discussion applies to the $E_1 + \Delta_1$ transitions. (2) The left side of Fig. 2 shows the evolution of the PR-D spectrum as the surface reconstruction changes from $c(4 \times 4)$ to (2×4). Spectrum (a) in Fig. 2 was obtained by subtracting the polarized spectrum in Fig. 1(a) from the unpolarized one in the same figure. Similarly spectrum (f) in Fig. 2 corresponds to the difference between the two spectra of Fig. 1(b). Spectrum (b) in Fig. 2 displays a lower amplitude

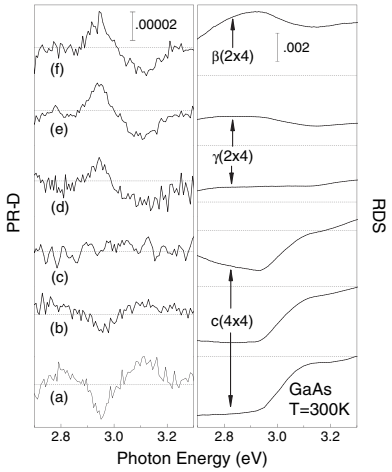

FIG. 2. PR-D spectra for (a) (4×4) (p-like) and (f) (2×4) (n-like) surface reconstructions. We show also PR-D spectra for surface reconstructions between (a) and (f). The right side of the figure displays the corresponding RD spectra for each PR-D spectra.

than spectrum (a), whereas spectrum (c) is fully quenched. The amplitude of spectra (d), (e), and (f) increases monotonically but with a sign opposite to that of spectra (a) and (b). (3) In spite of the inversion observed in the PR-D spectrum amplitude, the PR spectrum shows only a moderate modification upon changing the surface reconstruction. No change in amplitude is observed. (4) The right hand side of Fig. 2 shows the corresponding evolution of the RD spectrum. The evolution of both PR-D and RD spectra is similar and both invert amplitude upon change from $c(4 \times 4)$ to (2×4) reconstruction. However, the quenching of the PR-D spectrum occurs earlier than the quenching of the RD spectrum. (5) Once the direction of polarization of the probe light is known, the polarity of the surface electric field (i.e., the surface conductivity type) can be determined from the sign of the PR-D spectrum [1]. Following this approach, we found that the $c(4 \times 4)$ surface is p-like whereas the (2×4) surface is n-like.

Since the $c(4 \times 4)$ surface is richer in As than the (2×4) surface, we may expect it to be n-type. We found it, however, to be p-type, while the less As rich (2×4) surface resulted to be n-type. We thus conclude that the inversion observed in the PR-D spectrum amplitude cannot be explained on the basis of a change of surface conductivity. Furthermore, as the optical anisotropy observed in this Letter is associated with the bulk transitions E_1 and $E_1 + \Delta_1$, the dimerization-induced surface dipoles, located within the first atomic layers, cannot explain the observed spectrum inversion [13–15].

To explain the above observations it is necessary to postulate the existence of two regions with opposite electric fields. The electric field of both regions is modulated by the incident light, although not necessarily with the same amplitude. Depending on what region dominates the photoresponse, the PR-D spectrum amplitude would show either a positive or negative sign. The PR spectrum, in contrast, would exhibit only a moderate dependence on the specific region producing the photoresponse.

The explanation of the experimental observations is as follows. One contribution to the PR response is associated to the space-charge layer which, for the n-type film material, points away from the surface. This electric field is independent of the surface reconstruction. The other one is produced by surface reconstruction that induces an in-plane anisotropic strain field, e^s_{xy}, [16,17] which in turn produces a direct piezo-electric dipole (DPD). This strain field penetrates tens of monolayers in the crystal, thus perturbing the atomic positions in the region below the surface. The electric field associated to the DPD has a value of $F_d = e^s_{xy}(\sqrt{3}e_{14})/(\varepsilon_0 \varepsilon_r)$ along the [001] direction, where ε_0 is the permittivity of vacuum, ε_r the static dielectric constant, and e_{14} the piezo-electric coefficient. This strain-induced electric field changes direction when the reconstruction switches from $c(4 \times 4)$ to (2×4). Therefore, by changing the surface reconstruction the

strength of the total electric field can be modified and even made to reverse sign.

Figures 3(a) and 3(b) show the effect of a DPD on the band diagram for $c(4 \times 4)$ and (2×4) reconstructions, respectively. Band diagrams agree with experimental results as discussed below. The Fermi level is assumed to be pinned at the surface at an energy 0.55 eV above the valence band maximum, irrespective of either surface reconstruction [18] or the presence of a DPD. In the case of the $c(4 \times 4)$ surface the reconstruction strain induces a DPD electric field that opposes to that of the space-charge layer. Further, the DPD field is strong enough for the bands near the surface to bend downwards. The band diagram of Fig. 3(a) may be thought as resulting from two back-to-back barriers (I and II in Fig. 3(a)]. On the other hand, for the (2×4) surface the DPD field is in the same direction as that of the space-charge layer, thus resulting in the simpler band diagram shown in Fig. 3(b).

Photovoltaic effects leading to PR modulation may be described as follows. Let us consider the $c(4 \times 4)$ surface first. Upon illumination, photogenerated electrons are driven away either towards the surface or the bulk, while photogenerated holes are trapped between barriers I and II [Fig. 3(c)]. Photovoltages with opposite signs are thus generated in these two barriers. It is important to point out that for the QEO PR component the sign of the generated photovoltage is irrelevant and thus individual contributions of barriers I and II simply adds to the overall PR spectrum. In contrast, in the corresponding LEO PR each barrier component cancels out the other. In the case of the (2×4) surface, no peculiar photoeffects are expected and the surface barrier responds to incoming light in a way qualitatively similar to that of the simple surface barrier with no DPD field.

On the basis of the above model we may understand the evolution of the PR-D spectra shown in Fig. 2. For spectrum 2(a) the DPD field is strong enough for the PR response to be dominated by barrier I. Spectrum 2(b) displays a lower amplitude due to a reduction in reconstruction strain while for spectrum 2(c) this strain has been lowered to the point that the contribution of barrier I to the PR-D spectrum cancels out that of barrier II. Beyond this point contributions of barriers I and II have the same sign and thus the amplitude of the PR-D spectrum increases monotonically. It is important to note that while the PR-D spectrum of Fig. 2(d) exhibits structure, the structure of the corresponding RD spectrum is negligible, indicating that in this case the surface strain averages to zero. Thus, the PR-D spectrum of Fig. 2(d) is due only to the electric field induced by the space-charge region.

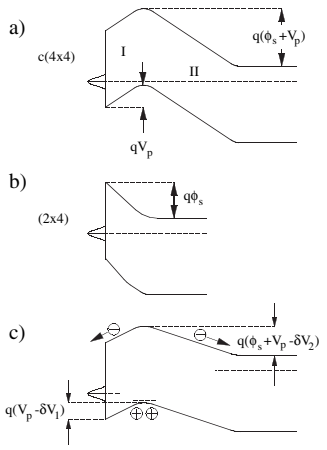

FIG. 3. Schematic band diagrams used to explain the experimental results. The surface strain bends the bands downwards for the $c(4 \times 4)$ and upwards for (2×4) reconstruction. ϕ_s is the surface potential and V_p is the DPD-induced barrier.

To estimate the surface strain and the surface electric field we have used the PR-D line shape in the region of the E_1 and $E_1 + \Delta_1$ transitions [9]:

$$\frac{\Delta R}{R} = \mathrm{Re}\Bigg[(\alpha - i\beta)\Bigg(r\frac{4D_3^5}{\sqrt{6}\Delta_1}\varepsilon(E, E_1 + \Delta E_{so} + \Delta E_h)d_{14}F + \frac{D_1^5}{2\sqrt{3}E^2}\frac{\partial E^2\varepsilon(E, E_1 + \Delta E_{so} + \Delta E_h)}{\partial E}d_{14}F\Bigg)\Bigg] + r\frac{4D_3^5}{\sqrt{6}\Delta_1}L(E, E_1 + \Delta E_{so} + \Delta E_h)e_{xy}^s + \frac{D_1^5}{2\sqrt{3}}\frac{\partial L(E, E_1 + \Delta E_{so} + \Delta E_h)}{\partial E}e_{xy}^s, \quad (1)$$

where α and β are the Seraphin coefficients, F the strength of the total electric field along the z axis, d_{14} the piezoelectric coefficient, D_1^5 the interband orthorhombic deformation potential for transitions of Λ symmetry, D_3^5 an orthorhombic deformation potential for the valence band, Δ_1 the spin orbit splitting energy for the valence band, and $r = +1(-1)$ refers to E_1 $(E_1 + \Delta_1)$. In Eq. (1), ε is the dielectric function of the sample and L the quadratic component of the PR, which is proportional to the third derivative of the dielectric function vs E [19]. ΔE_{so} and ΔE_h are defined in Ref. [9]. The first two terms of Eq. (1) correspond to the LEO component and the last two correspond to the QEO component.

The PR-D spectra of Fig. 2(f) can be understood by assuming a surface strain that leads to a QEO component. Taking into account that the amplitude of higher order derivative spectra (QEO terms) increases faster when the temperature decreases, we expect that the contribution of the surface strain to the PR-D spectrum becomes more important at low temperatures. Figure 4 shows the PR-D spectrum of Fig. 2(f) measured at $T = 150$ K. The optical structures shift to higher energies and are narrower than for the room temperature spectra. Using Eq. (1), the parameters defined in Refs. [20–22], the dielectric function, and the PR spectrum measured at $T = 150$ K, we have obtained the solid line of Fig. 4. The strength of the electric field and the surface strain were taken as fitting parameters.

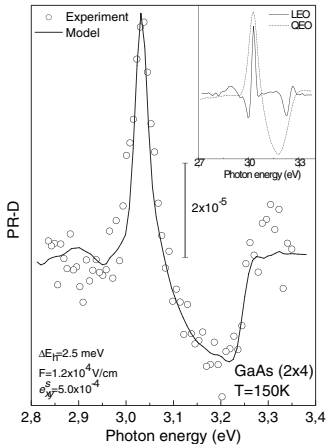

FIG. 4. PR-D at $T = 150$ K for a (2×4) surface of GaAs. The solid line represents the fit obtained with Eq. (1), taking F and e^s_{xy} as fitting parameters.

The inset of Fig. 4 shows the LEO and QEO components used to fit the PR-D spectrum. We can see that the main effects of the inclusion of a QEO component appear around E_1: the amplitude of this transition increases, and its broadening decreases. These features are crucial for the fit, because the LEO component around the E_1 transition is broader and has a smaller amplitude than the corresponding peak of the PR-D spectrum. The fit assuming only a LEO contribution is considerably poorer than the fit obtained by including both LEO and QEO. Note the excellent fit obtained in Fig. 4.

From the LEO component, we have obtained a value of $F = 1.2 \pm 0.1 \times 10^4$ V/cm. From the QEO component, we have obtained a value of $e^s_{xy} = 4.0 \pm 1.0 \times 10^{-4}$ which agrees reasonably with the value of 8.0×10^{-4} measured by x rays during the initial stage of recovery of the GaAs (001) $\beta(2 \times 4)$ reconstruction [23]. Additionally, by using the values of e^s_{xy}, $\varepsilon_0 = 8.85 \times 10^{-12}$ F/m, $\varepsilon_r = 12.5$, and $e_{14} = 0.16$ C/m^2, the calculated piezo-electric field is $F_d = 1.0 \pm 0.2 \times 10^4$ V/cm, of the same order of magnitude as the field obtained from the LEO amplitude. Thus, the effects on the PR-D spectra of both fields are comparable in magnitude, as postulated in our model. It is worth mentioning that the surface electric field can also be characterized by means of Franz-Keldysh oscillations in the PR spectra; however, it can be applied only to semiconductor structures with homogenous electric fields.

Finally, we point out that, in contrast to results for the (2×4) surface, the PR-D spectrum for the $c(4 \times 4)$ surface is barely seen at $T = 150$ K. This can be understood on the basis of the much larger impedance of barrier II as compared to barrier I. As we lower the temperature the difference in impedances becomes more important. Further, as a higher impedance implies a larger photovoltage, the relative contribution of barrier II to the overall PR-D spectrum becomes more important at lower temperatures, to the point that it cancels out the contribution of barrier I at $T = 150$ K.

In conclusion, the surface electric field and surface strain have opposite signs for the $c(4 \times 4)$ and (2×4) surface reconstructions of GaAs (001). We argue that the change of sign can be understood by assuming a direct piezo-electric effect induced by the reconstruction. Moreover, a quantitative estimate of the strain induced by reconstruction is given. The results reported here should become important in the characterization of surface and interface phenomena by means of modulated reflectance spectroscopies during the growth processes, gas adsorption, and metal deposition on zincblende semiconductors, among others. The main limitation of the method is that it is not applicable to nonpolar semiconductors.

We would like to thank G. Rodríguez-Pedroza and E. Ontiveros for assistance, and to Consejo Nacional de Ciencia y Tecnología for Grants No. 41248-F and No. 2003-C02(42594 and 49550).

*lflm@cactus.iico.uaslp.mx

[1] A. Lastras-Martínez *et al.*, Phys. Rev. B **59**, 10 234 (1999).
[2] A. Lastras-Martínez *et al.*, Phys. Status Solidi (a) **175**, 45 (1999).
[3] A. Lastras-Martínez *et al.*, J. Appl. Phys. **86**, 2062 (1999).
[4] L. F. Lastras-Martínez, R. E. Balderas-Navarro, A. Lastras-Martínez and K. Hingerl, Semicond. Sci. Technol. **19**, R35 (2004).
[5] I. Kamiya *et al.*, Phys. Rev. B **46**, 15 894 (1992).
[6] L. F. Lastras-Martínez *et al.*, Phys. Rev. B **64**, 245303 (2001).
[7] A. Ohtake *et al.*, Phys. Rev. Lett. **89**, 206102 (2002).
[8] D. E. Aspnes and A. A. Studna, Phys. Rev. Lett. **54**, 1956 (1985).
[9] L. F. Lastras-Martínez *et al.*, Phys. Rev. B **66**, 075315 (2002).
[10] D. E. Aspnes, Opt. Commun. **8**, 222 (1973).
[11] N. Esser *et al.*, J. Vac. Sci. Technol. B **13**, 1666 (1995).
[12] J. Menéndez and M. Cardona, Phys. Rev. B **31**, 3696 (1985).
[13] W. Chen *et al.*, J. Vac. Sci. Technol. B **10**, 1886 (1992).
[14] M. Sauvage-Simkin *et al.*, Phys. Rev. Lett. **62**, 563 (1989).
[15] T. Hashizume *et al.*, Phys. Rev. Lett. **73**, 2208 (1994).
[16] J. P. Silveira and F. Briones, J. Cryst. Growth **201–202**, 113 (1999).
[17] J. A. Appelbaum and D. R. Hamann, Surf. Sci. **74**, 21 (1978).
[18] W. Mönch, *Semiconductor Surface and Interfaces*, Springer Series in Surface Sciences Vol. 26 (Springer, New York, 1993), pp. 149, 2nd ed.
[19] D. E. Aspnes, in *Handbook of Semiconductors*, edited by M. Balkanski (North-Holland, Amsterdam, 1980), Vol. 2, p. 121.
[20] S. Adachi, J. Appl. Phys. **58**, R1 (1985).
[21] P. Etchegoin *et al.*, Phys. Rev. B **46**, 15 139 (1992).
[22] F. H. Pollak and M. Cardona, Phys. Rev. **172**, 816 (1968).
[23] V. M. Kaganer *et al.*, Phys. Rev. Lett. **90**, 016101 (2003).